Efficiency of solar wind energy coupling to the ionosphere

Jianpeng Guo,[1] Xueshang Feng,[1] Barbara A. Emery,[2] and Yi Wang[1]

Received 16 February 2012; revised 28 May 2012; accepted 3 June 2012; published 4 July 2012.

[1] We present a statistical investigation into the variations of the ionospheric energy coupling efficiencies with the solar wind energy input, the interplanetary magnetic field (IMF) clock angle and the solar wind dynamic pressure. The ionospheric energy coupling efficiencies are defined as the ratios of the ionospheric energy deposition (namely auroral precipitation, Joule heating, and their total) to the solar wind energy input. We find that the ionospheric energy coupling efficiencies decrease exponentially with the solar wind energy input. Moreover, it is the same case under geomagnetic storm conditions. Our results also show that the energy coupling efficiencies are dependent on the IMF clock angle and almost independent of the solar wind dynamic pressure. These results will help us estimate and predict energy transfer from the solar wind to the thermosphere-ionosphere system under extreme space weather conditions, particularly severe geomagnetic storms.

Citation: Guo, J., X. Feng, B. A. Emery, and Y. Wang (2012), Efficiency of solar wind energy coupling to the ionosphere, *J. Geophys. Res.*, *117*, A07303, doi:10.1029/2012JA017627.

1. Introduction

[2] A part of energy supplied to the magnetosphere from the solar wind is deposited in the auroral regions via particle precipitation and Joule heating. This high latitude energy input, along with solar EUV, governs the structure and dynamics of the ionosphere-thermosphere system [*Guo et al.*, 2010]. Generally, Joule heating dominates over particle precipitation as the main dissipation channel in the high-latitude ionosphere. The relative role of ionospheric dissipation in the global energy budget is an important issue. When *Perreault and Akasofu* [1978] derived the epsilon parameter, it was believed that only about 10% of the energy input would be dissipated through Joule heating and auroral precipitation, but this percentage has been gradually increasing [e.g., *Knipp et al.*, 1998; *Lu et al.*, 1998; *Turner et al.*, 2001; *Tanskanen et al.*, 2002]. Recent results of *Turner et al.* [2009] and *Guo et al.* [2011] show that ionospheric dissipation accounts for the vast majority of energy dissipation, with the ring current only being 10–13% of the total energy output.

[3] *Tanskanen et al.* [2002] found that for substorms they studied in the Northern Hemisphere, Joule dissipation accounted for about one third of the energy dissipation in solar minimum 1997 and about one fourth in 1999. Thus, Joule dissipation appears to cover a larger part of energy budget during quiet years than it does during active years, which leads us to an interesting question: Does the efficiency of the energy coupling between the solar wind and the ionosphere varies with various solar wind energy input? Several recent studies have found that a weaker driver leads to more effective energy coupling by analyzing the response of geomagnetic activity or magnetospheric and ionospheric activity to the solar wind driver [see, e.g., *Palmroth et al.*, 2007; *Pulkkinen et al.*, 2007]. Further analyzing and quantifying the role of the solar wind driver on solar wind-ionosphere energy coupling is a relatively new endeavor that requires ionospheric dissipation measurements. This paper will attempt to characterize the variations of the energy coupling efficiencies with solar wind energy input by computing the ratio of the ionospheric dissipation to the solar wind energy input. In addition, the interplanetary magnetic field (IMF) clock angle and solar wind dynamic pressure dependences of ionospheric energy coupling efficiencies are also investigated.

2. Methodology

2.1. Solar Wind Energy Input

[4] As there is no direct observational means of determining the energy input from the solar wind to the magnetosphere and thermosphere-ionosphere system, various solar wind-based coupling functions (parameters) have been developed [see, e.g., *Kan and Lee*, 1979; *Akasofu*, 1981; *Wygant et al.*, 1983; *Newell et al.*, 2007, and references therein; *Kivelson and Ridley*, 2008]. However, each parameter has been derived for a different purpose, and thus has slightly different properties tuned to give best results for the question addressed by the original authors. Moreover, the absolute magnitude of the parameters depends on how they were scaled. The Akasofu function (the epsilon parameter) was scaled to equal the amount of energy dissipated by the ring current and by the ionosphere (including Joule heating

[1]SIGMA Weather Group, State Key Laboratory of Space Weather, CSSAR, Chinese Academy of Sciences, Beijing, China.
[2]High Altitude Observatory, NCAR, Boulder, Colorado, USA.

Corresponding author: J. Guo, State Key Laboratory of Space Weather, CSSAR, Chinese Academy of Sciences, Beijing 100190, China. (jpguo@spaceweather.ac.cn)

0148-0227/12/2012JA017627

and auroral precipitation), which is most consistent with our purpose. Therefore, in this study, we choose the epsilon parameter (equation (1)) [*Akasofu*, 1981]:

$$\varepsilon(W) = \frac{4\pi}{\mu_0} v B^2 \sin^4\left(\frac{\theta}{2}\right) l_0^2 \quad (1)$$

The variables v, B, θ, l_0 on the right-hand side are given in SI units and denote the solar wind velocity, the solar wind magnetic field magnitude, the interplanetary magnetic field (IMF) clock angle, and the scaling factor, respectively. The scaling factor is empirically determined to be l_0 = 7 R_E [*Perreault and Akasofu*, 1978]. Considering the fact that the dayside magnetopause position varies with the solar wind dynamic pressure, we replace the effective cross-sectional area l_0^2 by R_{CF}^2, where $R_{CF} = (B_0/4\pi\rho v^2)^{1/6} R_E$, as obtained from a balance between the kinetic plasma and the magnetic pressure, with $B_0 \sim 0.3$ Gauss [see *Mac-Mahon and Gonzalez*, 1997]. The variables ρ and v are the mass density and velocity of the solar wind, respectively. The dynamic pressure-corrected energy input function (equation (2)) is

$$\varepsilon^*(W) = \left(\frac{R_{CF}}{l_0}\right)^2 \varepsilon. \quad (2)$$

So, we actually use the dynamic pressure-corrected Akasofu function to determine the solar wind energy input. The solar wind magnetic field and plasma parameters are available from the 1-h averaged OMNI database (GSM coordinates at 1 AU).

2.2. Ionospheric Dissipation

[5] To estimate the ionospheric dissipation (auroral precipitation and Joule heating), we use the same methodology as that in *Guo et al.* [2011]. In their study, Joule heating is estimated using relations derived by *Knipp et al.* [2004]. Global auroral precipitation estimates on a 1 h cadence are computed by using data from Defense Meteorological Satellite Program (DMSP) and National Oceanic and Atmospheric Administration (NOAA) satellites intercalibrated with each other by *Emery et al.* [2008, 2009]. NOAA satellites provide estimates of the total hemispheric power (HPt) from both electron and ion sensors for energies <20 keV while the DMSP satellites provide estimates of the electron hemispheric power (HPe) from the electron sensors for energies <20 keV ignoring the highest energy channel between 20.62 keV and 30.18 keV [*Emery et al.*, 2008]. The ion hemispheric power (HPi) is deduced from the NOAA satellites from the difference of the total and the electron hemispheric powers (HPi = HPt−HPe), and account for ∼10% of the total HPt [*Emery et al.*, 2008].

[6] In the present study, we calculate the global auroral ion (Pi) and electron (Pe) inputs from the sum of the hourly HPi and HPe estimates from each hemisphere, and confine ourselves to auroral energies <20 keV. *Emery et al.* [2006] found DMSP electron energy flux between 20.62 keV and 30.18 keV to be ∼5% of the total, increasing to as much as 12% for Kp 0. *Codrescu et al.* [1997] estimated the 30 keV to 2.5 MeV electron flux from the Medium Energy Proton and Electron Detector (MEPED) of NOAA satellites to vary between about 0.05 GW during quiet times to about 6.0 GW in active periods. This corresponds to about 1% to 10%, respectively, of the energy flux for electron energies below 20 keV from *Emery et al.* [2008, Table 3a]. Thus, electrons >20 keV are only expected to contribute ∼15% more energy flux than electrons <20 keV. However, the high energy component to Pi > 20 keV is estimated to be similar in magnitude to the component <20 keV for Kp > 3+ [*Fang et al.*, 2007; *Emery et al.*, 2008]. For lower Kp activities shown in *Fang et al.* [2007, Figures 1 and 9], the high energy component is ∼5–30% of the proton flux <20 keV for Kp < 1 and Kp ∼ 2, respectively. Since protons only account for ∼10% of the auroral energy flux, we do not anticipate any significant change in our results for auroral precipitation or ionospheric dissipation by ignoring electron and ion energies >20 keV. However, the fits for Pi could be increased in magnitude with the additional precipitation at larger values of epsilon.

2.3. Definition of the Ionospheric Energy Coupling Efficiency

[7] In this paper, we define three ionospheric energy coupling efficiencies as the ratios of the ionospheric energy deposition (namely auroral precipitation, Joule heating, and both auroral precipitation and Joule heating) to the solar wind energy input:

$$\text{Energy Efficiency} = \frac{\text{Ionospheric Dissipation}}{\text{Solar Wind Energy Input}}. \quad (3)$$

3. Results and Discussion

[8] As noted above, both solar wind energy input and ionospheric dissipation have been averaged to a time resolution of 1 h to better approximate a "steady state" energy coupling of ionosphere to solar wind. The data set used in this analysis spans 15 years (1995–2009) and consists of almost 131,500 1-h intervals. The three panels in Figure 1 show the number of data points within each 50 GW solar wind energy input bin, within each 10° IMF clock angle bin, and within each 0.5 nPa solar wind dynamic pressure bin respectively.

[9] Figure 2 shows the ionospheric energy coupling efficiencies as a function of the solar wind energy input rate represented by ε^*. Here we do not take into account the periods when ε^* > 1000 GW, since such periods are relatively rare and do not produce statistically meaningful results. Obviously, the energy coupling efficiencies decrease with the solar wind energy input rate. Moreover, the decreasing tendencies can be described by an exponential equation given by

$$f(x) = a\exp(bx) + c\exp(dx), \quad (4)$$

where a, b, c and d are the fit coefficients. Therefore, we suggest that the ionospheric energy coupling efficiencies fall off exponentially with the solar wind energy input. Note that there are some cases where the energy coupling efficiencies are greater than 1. This does not present a problem, as the energy coupling efficiencies are calculated by assuming that the correct solar wind energy input can be estimated by the dynamic pressure-corrected epsilon parameter. Previous analyses of energy output suggested that the epsilon parameter suffers from underestimations which can be corrected by scaling the parameter up by a factor of 1.5 to 2

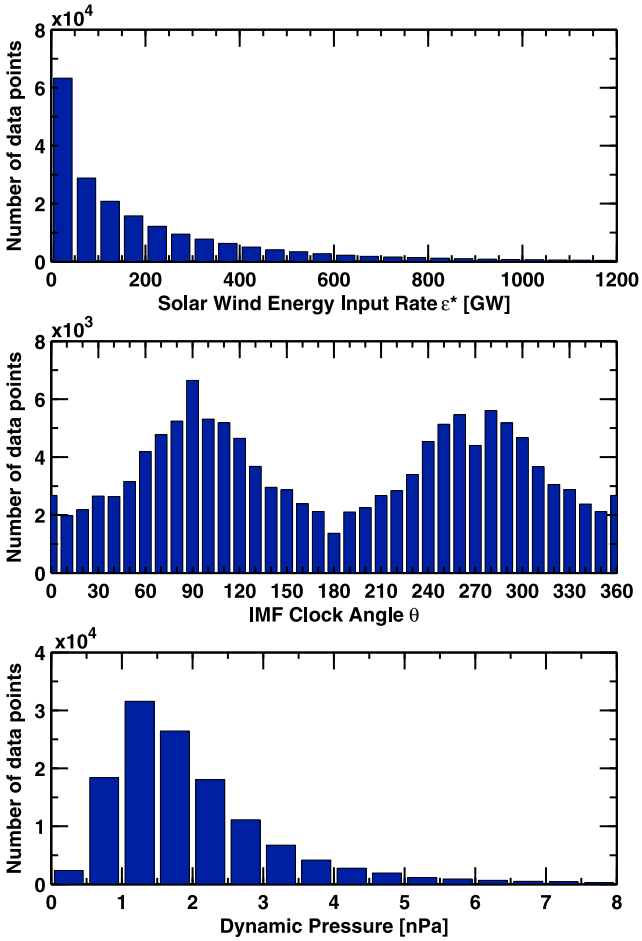

Figure 1. (top) Number of data points within each 50 GW solar wind energy input bin. (middle) Number of data points within each 10° IMF clock angle bin. (bottom) Number of data points within each 0.5 nPa solar wind dynamic pressure bin.

[e.g., *Koskinen and Tanskanen*, 2002]. We did not scale up the dynamic pressure-corrected epsilon, so the ionospheric energy coupling efficiencies in our calculation might be overestimated. However, this does not affect our results of the variations of the ionospheric energy coupling efficiencies with the solar wind energy input, as well as the IMF clock angle and dynamic pressure dependencies presented in Figure 5.

[10] We further investigate whether the coupling efficiencies still fall off exponentially under geomagnetic storm conditions. The storm events are selected from the list of 90 intense geomagnetic storms (Dst ≤ -100 nT) complied by *Zhang et al.* [2007], as well as 124 moderate geomagnetic storms (-100 nT < Dst ≤ -50 nT) collected by *Turner et al.* [2009] for a total of 214 storms. These storms cover the period from 1996 to 2006. For each storm, we estimate the energy input and the energy dissipated via Joule heating and auroral precipitation, and compute the integrated values of the energy input and dissipation beginning at the first decrease in Dst to when the Dst has recovered 80% from its lowest value. Then, we can calculate an ionospheric energy coupling efficiency according to its definition (equation (3)). The ionospheric energy coupling efficiencies versus the solar wind energy input for all 214 storms are shown in Figure 3. The plots demonstrate that the ionospheric energy coupling efficiencies also decrease exponentially with the solar wind energy input under geomagnetic storm conditions.

[11] In addition, it is interesting to investigate whether there is a difference between the efficiencies of solar wind energy coupling to global electron precipitation (Pe) and to ion precipitation (Pi). As shown in Figure 4 (left), the energy efficiencies of Pe and Pi fall off exponentially with the solar wind energy input rate. It is worth noting that the Pi energy efficiency decreases rapidly from 0.04 to 0.01 when the solar wind energy input rate is less than about 300 GW. This is because that there is more ion precipitation when the IMF orientation is close to northward with less solar wind energy input. Moreover, the ion precipitation increases strongly with increasing IMF Bz positive magnitude [*Emery et al.*, 2008]. Under geomagnetic storm conditions, the energy efficiencies of Pe and Pi also decrease exponentially with the solar wind energy input, which are illustrated in Figure 4 (right).

[12] Overall, our results show that the ionospheric energy coupling efficiencies significantly depend on the solar wind energy input, and they tend to be lower when the solar wind energy input increases. This is consistent with the results of *Nakai and Kamide* [1999] and *Nagatsuma* [2006]. They found that the coupling efficiencies between solar wind parameters and geomagnetic indices during periods of high solar activity tend to be lower than those during periods of low solar activity. Moreover, *Nagatsuma* [2006] proposed that the variation of total Pedersen conductivity on both northern and southern polar caps can explain the solar activity dependence of the solar wind coupling efficiencies of geomagnetic indices. Furthermore, *Wang and Lühr* [2007] suggested that the ionospheric Pedersen conductivity has a significant influence on the trigger level of a substorm. A smaller Pedersen conductivity may decrease the substorm trigger level and increase the number of substorms. As we know, substorms represent a significant dissipation of energy in an explosive reconfiguration process. The major portion of the energy dissipates into the high latitude ionosphere through Joule heating and auroral precipitation. The immediate consequence of this is the increase in the ionospheric energy coupling efficiencies. Therefore, we argue that our results are not inconsistent with the hypothesis that the Pedersen conductivity may play a key role in the solar wind dependence of the coupling efficiencies. In addition, our results may imply that the energy dissipated via magnetospheric processes (such as ring current, plasmoid and plasma sheet heating) or lost back to the solar wind might grow more quickly as the solar wind energy input increases.

[13] We also examine dependences of the ionospheric energy coupling efficiencies on the IMF clock angle as well as solar wind dynamic pressure, and the results are shown in Figure 5. Note we do not take into account the periods when the dynamic pressure is larger than 5 nPa, since such periods are relatively rare and do not produce statistically meaningful results. As we can see, the ionospheric energy coupling efficiencies vary with IMF clock angle, with the peaks around $\theta = 60°$ and $\theta = 300°$, and the minimum when $\theta = 180°$. This indicates that the energy deposited in the high-latitude ionosphere reaches its maximum when the IMF is southward ($\theta = 180°$), while its minimum appears when

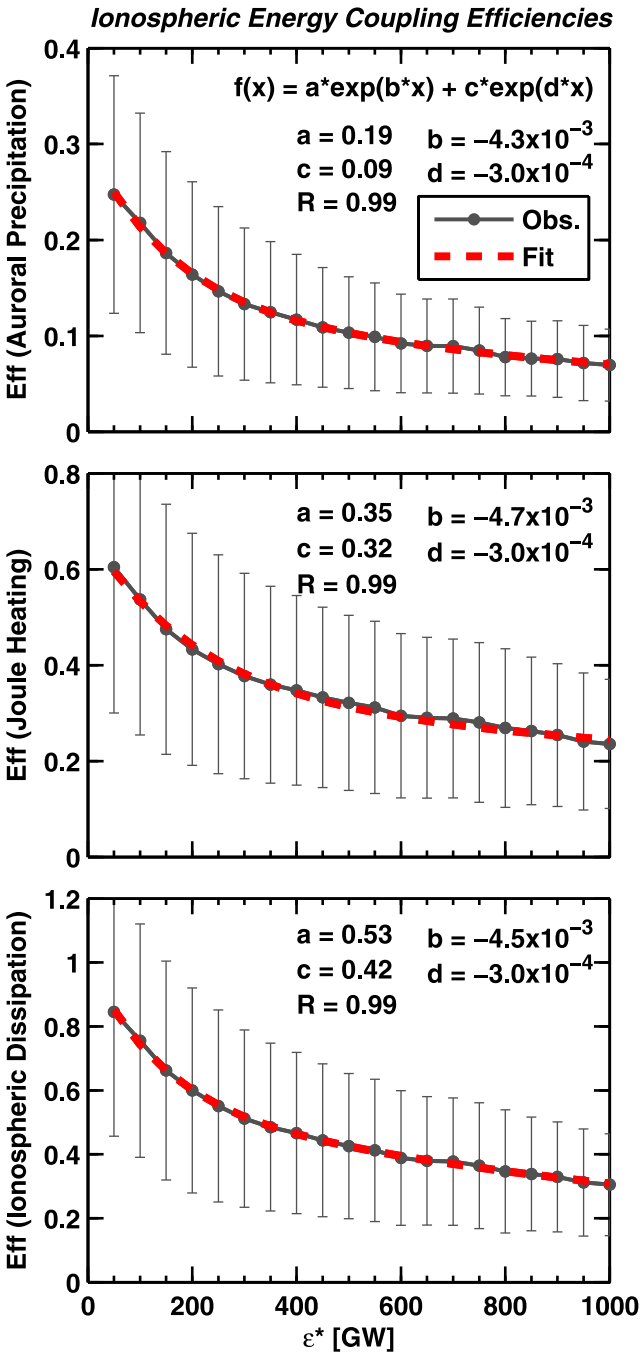

Figure 2. The ionospheric energy coupling efficiencies for the total global auroral precipitation (Pt = Pe + Pi) < 20 keV, the estimated global Joule Heating, and the sum of both, versus the solar wind energy input rate represented by ε^* in bins of 50 GW. The vertical bars denote the ±1 standard deviation. The exponential fit results are also superimposed on each one.

the clock angle is close to 60° and 300°. Although one might expect the minimum Joule heat and particle precipitation to be located at times when the IMF is northward ($\theta = 0°$), J. Guo et al. (manuscript in preparation, 2012) show that there is a slight increase in the Joule heating and in the electron precipitation at $\theta = 0°$, and a relatively large increase in the ion precipitation. The ionospheric energy coupling efficiencies are almost independent of the solar wind dynamic pressure, and are typical of ε^* around 100–150 GW

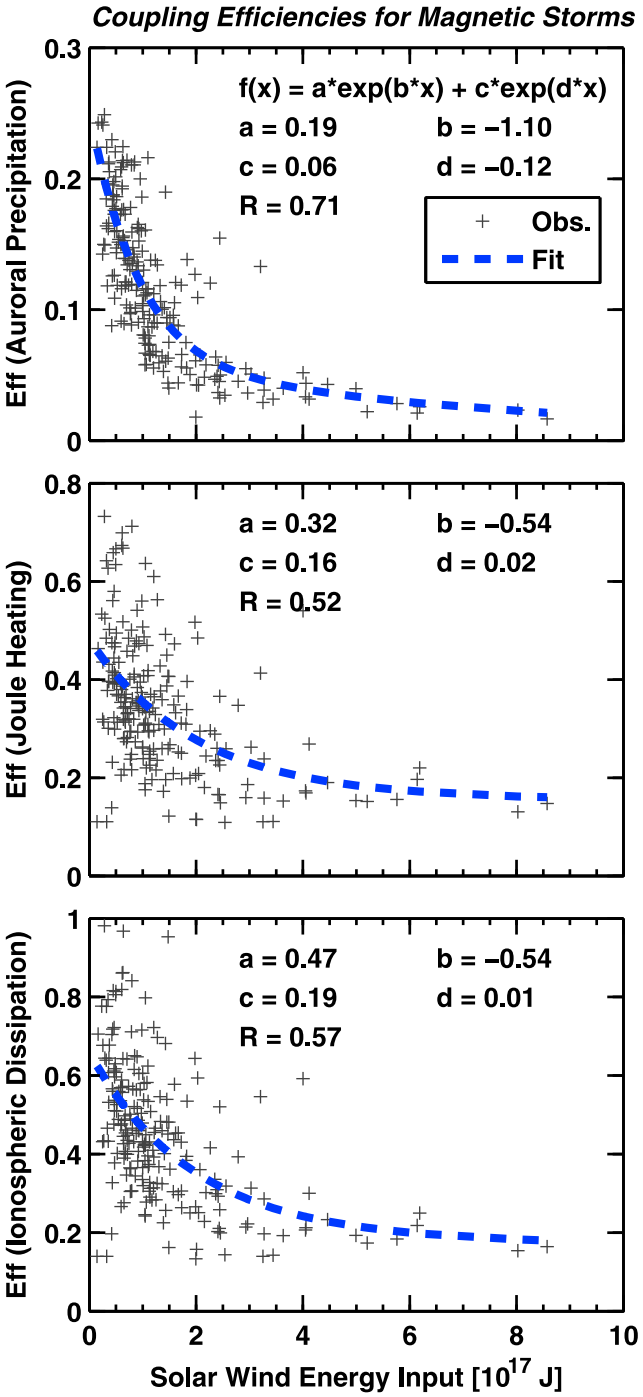

Figure 3. The ionospheric energy coupling efficiencies versus the solar wind energy input for 214 geomagnetic storms. Note that each storm is considered to begin at the first decrease in Dst and end when the Dst has recovered 80% from its lowest value. The exponential fit results are also superimposed on each one.

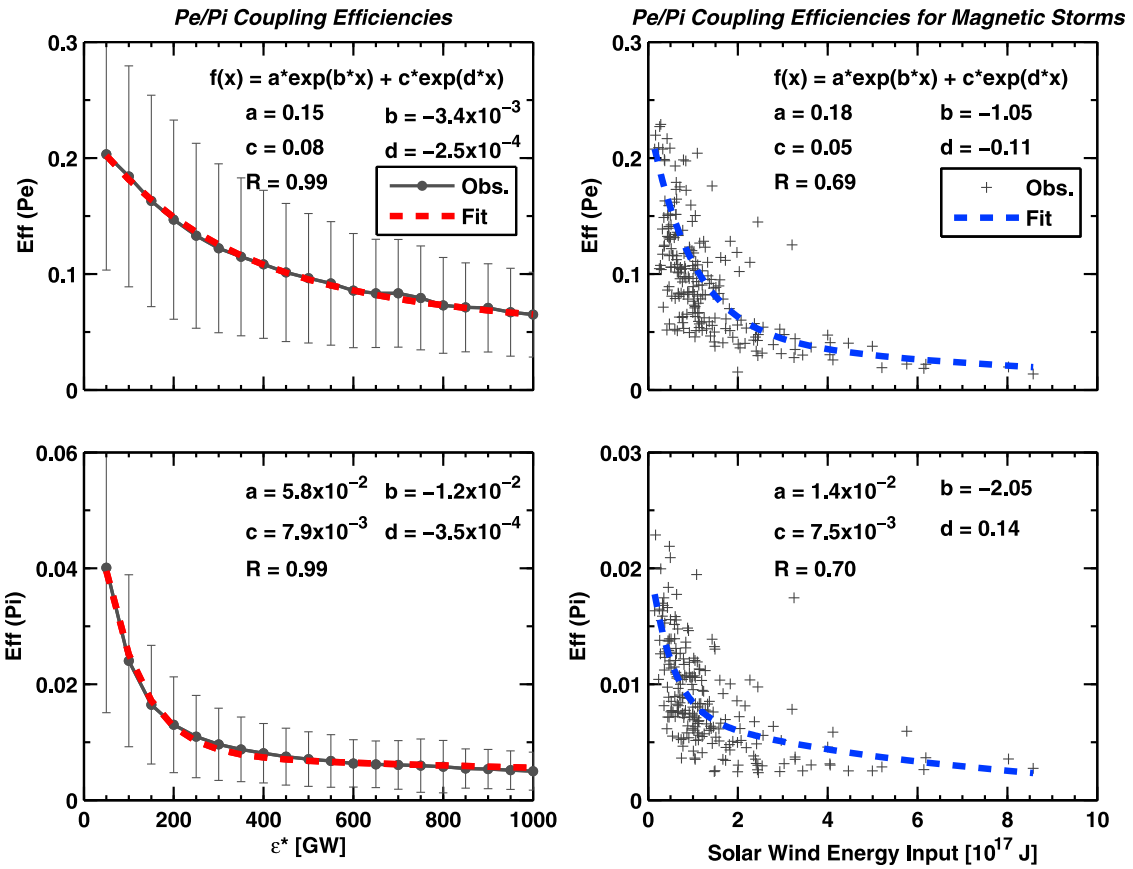

Figure 4. (left) Same as Figure 2 but for global auroral electron (Pe) and ion (Pi) inputs. (right) Same as Figure 3 but for Pe and Pi.

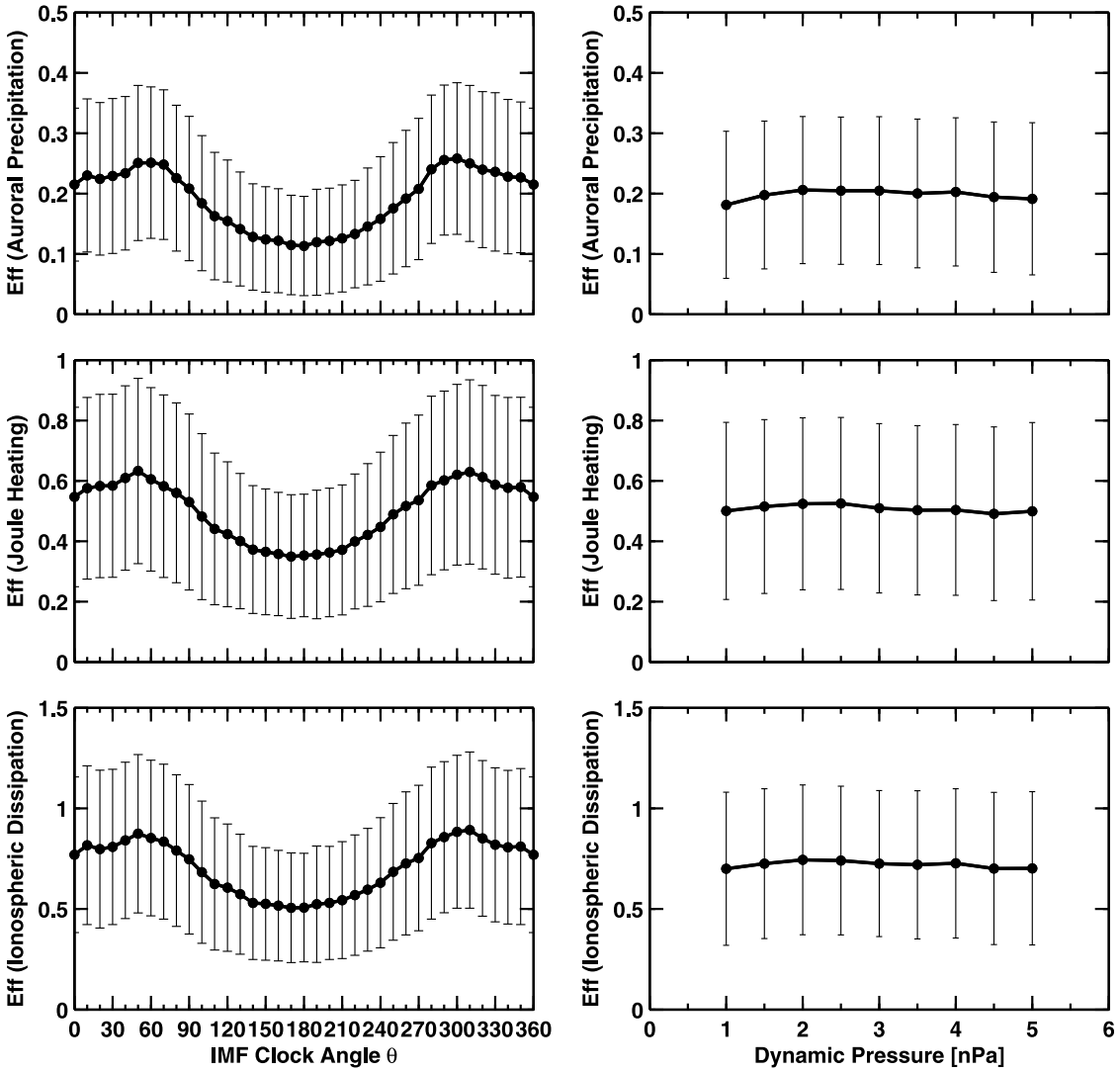

Figure 5. The ionospheric energy coupling efficiencies versus the (left) IMF clock angle in bins of 10° and the (right) solar wind dynamic pressure in bins of 1 nPa. The vertical bars denote the ±1 standard deviation.

(cf. Figure 2). It should be particularly noted that this conclusion is reached by analyzing the "steady state" energy coupling of the ionosphere to solar wind over 1 h. In fact, solar wind dynamic pressure has a role in ionospheric dynamics [see, e.g., *Zesta et al.*, 2000; *Shue and Kamide*, 2001; *Palmroth et al.*, 2004; *Boudouridis et al.*, 2005]. *Palmroth et al.* [2007] investigated the solar wind-magnetosphere coupling efficiency in response to solar wind dynamic pressure impulses, and found that the coupling efficiency increases (decreases) for decreasing (increasing) IMF impulses. They also found that, if the statistical analysis is carried out for the entire length of pressure impulses without grouping according to the impulse structure, the coupling efficiency is constant in time. Hence, they concluded that it is the property of the pressure impulse itself that determines the magnetospheric and ionospheric response. However, due to restrictions of time resolution for the ionospheric energy deposition, we could not investigate the role of solar wind dynamic pressure impulses on the ionospheric energy coupling efficiencies.

4. Summary

[14] We have investigated the variations of the ionospheric energy coupling efficiencies with the solar wind energy input, the interplanetary magnetic field (IMF) clock angle and the solar wind dynamic pressure. The ionospheric energy coupling efficiencies are defined as the ratios of the ionospheric energy deposition (namely auroral precipitation, Joule heating, and both auroral precipitation and Joule heating) to the solar wind energy input. We find that the ionospheric energy coupling efficiencies decrease exponentially with the solar wind energy input. Moreover, such an exponential decrease is still true under geomagnetic storm conditions. This result has two important implications. First, under circumstances of tremendous solar wind energy input

or severe geomagnetic storm conditions, there seems to be a limit to how much energy can be dissipated via auroral precipitation and Joule heating. Second, even during less active periods, the energy deposited in the ionosphere might be sufficient to cause significant disturbances in the thermosphere-ionosphere system because of the relatively high coupling efficiency compared to active periods. Our results also show that the ionospheric energy coupling efficiencies are dependent on the IMF clock angle and almost independent of the solar wind dynamic pressure.

[15] **Acknowledgments.** The authors thank the referees for their valuable suggestions to improve the paper. This work is jointly supported by the Chinese Academy of Sciences (KZZD-EW-01-4), the 973 program (2012CB825601), the National Natural Science Foundation of China (40921063, 40890162, 41031066, 40904049, and 41004082), and the Specialized Research Fund for State Key Laboratories. Intersatellite calibration work by Barbara Emery at the National Center for Atmospheric Research is supported by the National Science Foundation. The OMNI solar wind database is compiled by the Space Physics Data Facility at the Goddard Space Flight Center (http://omniweb.gsfc.nasa.gov/). The geomagnetic data are obtained through the World Data Center in Kyoto. The original DMSP and NOAA satellite auroral hemispheric power estimates were provided by the USAF Research Laboratory, Hanscom AFB, Mass., and by the Space Weather Prediction Center, Boulder, Colo., via the Coupling, Energetics and Dynamics of Atmospheric Regions (CEDAR) Database, which is supported by the National Science Foundation. NOAA electron hemispheric powers, which can infer ion hemispheric powers from the total, were supplied by David S. Evans of the Space Weather Prediction Center at the National Oceanic and Atmospheric Administration (NOAA).

[16] Philippa Browning thanks the reviewers for their assistance in evaluating this paper.

References

Akasofu, S.-I. (1981), Energy coupling between the solar wind and the magnetosphere, *Space Sci. Rev.*, *28*, 121–190, doi:10.1007/BF00218810.

Boudouridis, A., E. Zesta, L. R. Lyons, P. C. Anderson, and D. Lummerzheim (2005), Enhanced solar wind geoeffectiveness after a sudden increase in dynamic pressure during southward IMF orientation, *J. Geophys. Res.*, *110*, A05214, doi:10.1029/2004JA010704.

Codrescu, M. V., T. J. Fuller-Rowell, R. G. Roble, and D. S. Evans (1997), Medium energy particle precipitation influences on the mesosphere and lower thermosphere, *J. Geophys. Res.*, *102*(A9), 19,977–19,987, doi:10.1029/97JA01728.

Emery, B. A., D. S. Evans, M. S. Greer, E. Holeman, K. Kadinsky-Cade, F. J. Rich, and W. Xu (2006), The low energy auroral electron and ion hemispheric power after NOAA and DMSP intersatellite adjustments, *Tech. Note NCAR/TN-470+STR*, Natl. Cent. for Atmos. Res., Boulder, Colo. [Available at http://cedarweb.hao.ucar.edu/wiki/index.php/Media:Str470.pdf.]

Emery, B. A., V. Coumans, D. S. Evans, G. A. Germany, M. S. Greer, E. Holeman, K. Kadinsky-Cade, R. J. Rich, and W. Xu (2008), Seasonal, Kp, solar wind, and solar flux variations in long-term single-pass satellite estimates of electron and ion auroral hemispheric power, *J. Geophys. Res.*, *113*, A06311, doi:10.1029/2007JA012866.

Emery, B. A., I. G. Richardson, D. S. Evans, R. J. Rich, and W. Xu (2009), Solar wind structure sources and periodicities of global electron hemispheric power over three solar cycles, *J. Atmos. Sol. Terr. Phys.*, *71*, 1157–1175, doi:10.1016/j.jastp.2008.08.005.

Fang, X., M. W. Liemohn, J. U. Kozyra, D. S. Evans, A. D. DeJong, and B. A. Emery (2007), Global 30–240 keV proton precipitation in the 17–18 April 2002 geomagnetic storms: 1. Patterns, *J. Geophys. Res.*, *112*, A05301, doi:10.1029/2006JA011867.

Guo, J., X. Feng, J. M. Forbes, J. Lei, J. Zhang, and C. Tan (2010), On the relationship between thermosphere density and solar wind parameters during intense geomagnetic storms, *J. Geophys. Res.*, *115*, A12335, doi:10.1029/2010JA015971.

Guo, J., X. Feng, B. A. Emery, J. Zhang, C. Xiang, F. Shen, and W. Song (2011), Energy transfer during intense geomagnetic storms driven by interplanetary coronal mass ejections and their sheath regions, *J. Geophys. Res.*, *116*, A05106, doi:10.1029/2011JA016490.

Kan, J. R., and L. C. Lee (1979), Energy coupling and the solar wind dynamo, *Geophys. Res. Lett.*, *6*, 577–580, doi:10.1029/GL006i007p00577.

Kivelson, M. G., and A. J. Ridley (2008), Saturation of the polar cap potential: Inference from Alfvén wing arguments, *J. Geophys. Res.*, *113*, A05214, doi:10.1029/2007JA012302.

Knipp, D. J., et al. (1998), An overview of the early November 1993 geomagnetic storm, *J. Geophys. Res.*, *103*, 26,197–26,220, doi:10.1029/98JA00762.

Knipp, D. J., W. K. Tobiska, and B. A. Emery (2004), Direct and indirect thermospheric heating sources for solar cycles 21–23, *Sol. Phys.*, *224*, 495–505, doi:10.1007/s11207-005-6393-4.

Koskinen, H. E. J., and E. Tanskanen (2002), Magnetospheric energy budget and the epsilon parameter, *J. Geophys. Res.*, *107*(A11), 1415, doi:10.1029/2002JA009283.

Lu, G., et al. (1998), Global energy deposition during the January 1997 magnetic cloud event, *J. Geophys. Res.*, *103*, 11,685–11,694, doi:10.1029/98JA00897.

Mac-Mahon, R. M., and W. D. Gonzalez (1997), Energetics during the main phase of geomagnetic superstorms, *J. Geophys. Res.*, *102*(A7), 14,199–14,207, doi:10.1029/97JA01151.

Nagatsuma, T. (2006), Diurnal, semiannual, and solar cycle variations of solar wind–magnetosphere–ionosphere coupling, *J. Geophys. Res.*, *111*, A09202, doi:10.1029/2005JA011122.

Nakai, H., and Y. Kamide (1999), Solar cycle variations in the storm-substorm relationship, *J. Geophys. Res.*, *104*, 22,695–22,700, doi:10.1029/1999JA900278.

Newell, P. T., T. Sotirelis, K. Liou, C.-I. Meng, and F. J. Rich (2007), A nearly universal solar wind-magnetosphere coupling function inferred from 10 magnetospheric state variables, *J. Geophys. Res.*, *112*, A01206, doi:10.1029/2006JA012015.

Palmroth, M., P. Janhunen, T. I. Pulkkinen, and H. E. J. Koskinen (2004), Ionospheric energy input as a function of solar wind parameters: Global MHD simulation results, *Ann. Geophys.*, *22*, 549–566, doi:10.5194/angeo-22-549-2004.

Palmroth, M., N. Partamies, J. Polvi, T. I. Pulkkinen, D. J. McComas, R. J. Barnes, P. Stauning, C. W. Smith, H. J. Singer, and R. Vainio (2007), Solar wind-magnetosphere coupling efficiency for solar wind pressure impulses, *Geophys. Res. Lett.*, *34*, L11101, doi:10.1029/2006GL029059.

Perreault, P., and S.-I. Akasofu (1978), A study of geomagnetic storms, *Geophys. J. R. Astron. Soc.*, *54*, 547–573, doi:10.1111/j.1365-246X.1978.tb05494.x.

Pulkkinen, T. I., N. Partamies, R. L. McPherron, M. Henderson, G. D. Reeves, M. F. Thomsen, and H. J. Singer (2007), Comparative statistical analysis of storm time activations and sawtooth events, *J. Geophys. Res.*, *112*, A01205, doi:10.1029/2006JA012024.

Shue, J.-H., and Y. Kamide (2001), Effects of solar wind density on auroral electrojets, *Geophys. Res. Lett.*, *28*, 2181–2184, doi:10.1029/2000GL012858.

Tanskanen, E., T. I. Pulkkinen, H. E. J. Koskinen, and J. A. Slavin (2002), Substorm energy budget during low and high solar activity: 1997 and 1999 compared, *J. Geophys. Res.*, *107*(A6), 1086, doi:10.1029/2001JA900153.

Turner, N. E., D. N. Baker, T. I. Pulkkinen, J. L. Roeder, J. F. Fennell, and V. K. Jordanova (2001), Energy content in the storm time ring current, *J. Geophys. Res.*, *106*, 19,149–19,156, doi:10.1029/2000JA003025.

Turner, N. E., W. D. Cramer, S. K. Earles, and B. A. Emery (2009), Geoefficiency and energy partitioning in CIR-driven and CME-driven storms, *J. Atmos. Sol. Terr. Phys.*, *71*, 1023–1031, doi:10.1016/j.jastp.2009.02.005.

Wang, H., and H. Lühr (2007), Seasonal-longitudinal variation of substorm occurrence frequency: Evidence for ionospheric control, *Geophys. Res. Lett.*, *34*, L07104, doi:10.1029/2007GL029423.

Wygant, J. R., R. B. Torbert, and F. S. Mozer (1983), Comparison of S3–3 polar cap potential drops with the interplanetary magnetic field and models of magnetopause reconnection, *J. Geophys. Res.*, *88*, 5727–5735, doi:10.1029/JA088iA07p05727.

Zesta, E., H. J. Singer, D. Lummerzheim, C. T. Russell, L. R. Lyons, and M. J. Brittnacher (2000), The effect of the January 10, 1997, pressure pulse on the magnetosphere-ionosphere current system, in *Magnetospheric Current Systems*, *Geophys. Monogr. Ser.*, vol. 118, edited by S.-I. Ohtani et al., pp. 217–226, AGU, Washington, D. C., doi:10.1029/GM118p0217

Zhang, J., et al. (2007), Solar and interplanetary sources of major geomagnetic storms ($Dst \leq -100$ nT) during 1996–2005, *J. Geophys. Res.*, *112*, A10102, doi:10.1029/2007JA012321.